Pelagic *Sargassum* in the Gulf of Mexico driven by ocean currents and eddies

Yingjun Zhang[1], Chuanmin Hu[1*], Dennis J. McGillicuddy, Jr.[2], Brian B. Barnes[1], Yonggang Liu[1], Vassiliki H. Kourafalou[3], Shuai Zhang[1], Frank J. Hernandez[4]

[1] College of Marine Science, University of South Florida, St. Petersburg, FL, United States

[2] Department of Applied Ocean Physics and Engineering, Woods Hole Oceanographic Institution, Woods Hole, MA, United States

[3] Rosenstiel School of Marine and Atmospheric Science, University of Miami, Miami, FL, United States

[4] Southeast Fisheries Science Center, National Marine Fisheries Service, NOAA, Pascagoula, MS, United States

*Corresponding Author: Chuanmin Hu (Email: huc@usf.edu); College of Marine Science, University of South Florida, 140 7th Ave. South, St. Petersburg, FL 33701

Highlights

1. Two source regions of pelagic *Sargassum* in the Gulf of Mexico (GoM) are revealed
2. GoM *Sargassum* can originate from either the GoM interior or the Caribbean Sea
3. The Loop Current System and eddies strongly impact *Sargassum* distributions
4. *Sargassum* around Florida lags those near the Yucatan by about one month

Abstract

Pelagic *Sargassum* in the Gulf of Mexico (GoM) plays an important role in ocean biology and ecology, yet our knowledge of its origins and transport pathways is limited. Here, using satellite observations of *Sargassum* areal density and ocean surface currents between 2000 and 2023, we show that large amounts of *Sargassum* in the GoM can either originate from the northwestern GoM or be a result of physical transport from the northwestern Caribbean Sea, both with specific transport pathways. *Sargassum* of the northwestern GoM can be transported to the eastern GoM by ocean currents and eddies, eventually entering the Sargasso Sea. *Sargassum* entering the GoM from the northwestern Caribbean Sea can be transported in three different directions, with the northward and eastward transports governed by the Loop Current System (LCS) and westward transport driven by the westward extension of the LCS, the propagation or relaying of ocean eddies, the wind-driven westward currents on the Campeche Bank with or without eddies, and the westward currents with/without currents associated with eddies in the northern/central GoM. Overall, the spatial distribution patterns of pelagic *Sargassum* in the GoM are strongly influenced by the LCS and relevant eddies.

Keywords

Sargassum, Gulf of Mexico, Caribbean Sea, Loop Current System, ocean currents, satellite observation

1. Introduction

The Gulf of Mexico (GoM, Fig. 1a) is characterized by a wide range of habitats and relatively high biodiversity (e.g., Chen, 2017), with over 15,000 recorded species representing over 40 phyla (Felder et al., 2009). Among the most speciose communities are those associated with holopelagic *Sargassum* (*S.*

natans and *S. fluitans*) macroalgae (Gower et al., 2006; Gower and King, 2011, 2020; Doyle and Franks, 2015; Hu et al., 2016a, 2016b; Siuda et al., 2016; Martin et al., 2021; Fig. 1b). These seaweeds provide essential habitat and food sources for marine animals such as crabs, fish, shrimps, turtles, and sea birds (Wells and Rooker, 2004; Casazza and Ross, 2008; Witherington et al., 2012; Sanchez-Rubio et al., 2018). In addition, *Sargassum* may have far-reaching impacts on nutrient remineralization and primary productivity (Hu et al., 2021; Lapointe et al., 2021; McGillicuddy et al., 2023), as well as the potential to serve as raw materials for the production of biofuels and pharmaceutical products (Milledge et al., 2016; Amador-Castro et al., 2021; Orozco-González et al., 2022). In spite of these potential benefits, large *Sargassum* beaching events can have deleterious effects on human health, local tourism and economies, and coastal ecosystems (e.g., Smetacek and Zingone, 2013; Webster and Linton, 2013; Siuda et al., 2016; Van Tussenbroek et al., 2017; Gower and King, 2019).

To date, our understanding of the origins and transport pathways affecting the spatial distributions of GoM *Sargassum* is limited. Based on the sequential monthly maps of *Sargassum* population in the GoM and north Atlantic Ocean, derived from Medium Resolution Imaging Spectrometer (MERIS) satellite measurements between 2002 and 2008, Gower and King (2011) showed that *Sargassum* developed locally in the northwestern GoM in spring, and was then transported to the southeastern GoM and north Atlantic Ocean in summer and fall through major ocean currents such as the Loop Current (LC), Florida Current (FC), and Gulf Stream (see the schematic diagram of these ocean currents in Fig. 1a). More recent satellite observations suggest a new source region in the tropical Atlantic (e.g., Gower et al., 2013; Wang and Hu, 2017; Wang et al., 2019; Gower and King, 2020), which could deliver large amounts of *Sargassum* to the GoM. Satellite imagery from the *Sargassum* Watch System (SaWS, Hu et al., 2016b; https://optics.marine.usf.edu/projects/saws.html) revealed that *Sargassum* in the Caribbean Sea could be

transported to the GoM, yet it is unclear how the transport of *Sargassum* within the GoM is influenced by major ocean currents and eddies.

The objectives of this study are to explore the origins of *Sargassum* in the GoM and to investigate the mechanisms impacting the transport and spatial distributions of GoM *Sargassum*. This is achieved through analyzing the satellite-derived *Sargassum* distributions in the context of ocean surface currents and eddies.

2. Data and Methods

Weekly 0.1° × 0.1° *Sargassum* areal density maps from February 2000 to June 2023 were derived from daily Moderate Resolution Imaging Spectroradiometer (MODIS) measurements (from both Terra and Aqua satellites) using the method described in Wang and Hu (2016), with images available through the SaWS (Hu et al., 2016b; https://optics.marine.usf.edu/projects/saws.html). Briefly, each image pixel (about 1 km in size) during a week within a grid was classified to be either *Sargassum* containing, *Sargassum* free, or invalid (due to either clouds, sun glint, straylight, or other factors). This determination was based on an algorithm to quantify the pixel's "red-edge" reflectance (i.e., enhanced reflectance in the near infrared wavelengths; Wang and Hu, 2016) and specific image processing methods to remove noise. The spectral shapes of some randomly selected *Sargassum*-containing pixels were inspected to confirm presence of *Sargassum* instead of other possible floating matters (e.g., *Trichodesmium*), using a spectra-differencing technique demonstrated by Qi et al. (2020). Basically, for MODIS, the difference spectra between the *Sargassum*-containing pixel and nearby water pixel showed elevated reflectance around 645 nm without the spectral "wiggling" features in the blue-green wavelengths due to pigments specific to *Trichodesmium* (Hu et al., 2010). For the Ocean Colour and Land Imager (OLCI), similar elevated reflectance was observed around 620 nm for both *Sargassum* and *Trichodesmiumm* pixels, but

the latter showed relatively higher reflectance at 510 nm than the former (Qi et al., 2020). Once the randomly selected pixels were confirmed to be dominated by *Sargassum*, all classified image features were assumed to contain *Sargassum*.

Each *Sargassum*-containing pixel was quantified for its areal density (0%–100%) using lower and upper bound threshold values established through field measurements and image statistics. The mean areal density for a grid within a week was defined as the arithmetic mean of all *Sargassum*-containing and *Sargassum*-free pixels, with each pixel contributing 0%-100%. Because the areal density is proportional to biomass density with a mean conversion factor of 3.34 kg wet biomass m^{-2} (Wang et al., 2018), the areal density and biomass density are used interchangeably in this study.

Daily 0.25° × 0.25° altimetry-based ocean surface geostrophic current data between February 2000 and June 2023, provided by the Copernicus Marine Environment Monitoring Service (CMEMS, https://marine.copernicus.eu/), were used to analyze the spatial distributions and temporal variability of ocean surface currents and mesoscale eddies in the GoM. This product provides an important source of observations for surface ocean circulation studies (Vignudelli et al., 2016). It has global coverage, but only data for the GoM were used here. In addition, data before August 2021 are in delayed-time mode, while the data are in near-real-time mode thereafter. This product has been widely used in previous GoM ocean circulation studies and other relevant studies (e.g., Alvera-Azcarate et al., 2009; Liu et al., 2014, 2016; Weisberg et al., 2016; Zhu and Liang, 2020; Zhang Y. et al., 2022; Zhang et al., 2023). Daily data were averaged to generate weekly maps to match the time frame of *Sargassum* maps.

3. Results

The distribution map of mean *Sargassum* areal density during April–September of 2011–2020 (Fig. 1b), shows *Sargassum* nearly everywhere in the GoM, with more *Sargassum* in the northwestern GoM and

along the LC edges than in other locations. Such a distribution can be explained in the context of ocean circulation patterns and their variations. Examination of the combined *Sargassum* areal density and ocean current maps revealed multiple pathways of *Sargassum* transport that affected *Sargassum* distributions in the GoM. These pathways are broadly characterized into two categories: 1) local *Sargassum* origin (i.e., from within the GoM) and 2) remote *Sargassum* origin (i.e., from outside the GoM), and they are schematically illustrated in Fig. 2.

The first category (local origin in the northwestern GoM) has already been discussed by Gower and King (2011), where sequential monthly maps of *Sargassum* population in the GoM and north Atlantic Ocean, derived from MERIS satellite observations during 2002–2008, were used to infer the eastward transport of *Sargassum* via the LC and FC. Here, the image sequence in Fig. 3 clearly shows the progression of the eastward movement of *Sargassum* during May and June 2014. The continuous evolution of *Sargassum*'s eastward movement within the GoM can also be seen from an animation provided in the Supporting Information. The year of 2014 was selected here because this is the year during which large amounts of *Sargassum* were first found in the northwestern GoM between May and early June (Figs. 3a–3c), while the eastern GoM showed limited amounts and the northwestern Caribbean Sea showed nearly no *Sargassum*. During this period, *Sargassum* biomass density in the area north of the Loop Current System (LCS; box 2 in Fig. 3) increased over time. By mid–late June, *Sargassum* amount on the West Florida Shelf also increased (box 3 in Fig. 3). The combined *Sargassum* and ocean surface current maps prior to spring 2014 revealed nearly no *Sargassum* in the Caribbean Sea between November 2012 and May 2014 (figures not shown here), suggesting that the large amount of *Sargassum* in the northwestern GoM appear to have originated from the northwestern GoM interior, and then been transported to the eastern GoM and eventually to the north Atlantic Ocean. Such observations confirm the hypothesis proposed by Gower and King (2011).

In the 2014 case, the transport of *Sargassum* from the northwestern GoM to the eastern GoM was mainly driven by ocean currents and eddies, as schematically shown in Fig. 2a. Specifically, the anticyclonic eddies and eastward currents inside box 1 of Fig. 3 helped transport *Sargassum* from west to east, and the LC, anticyclonic eddies, and other eastward currents in box 2 of Fig. 3 also facilitated the eastward transport of *Sargassum*. After reaching the eastern boundary of box 2, *Sargassum* was further transported southeastward on the West Florida Shelf through the southeastward currents (annotated with yellow arrows in box 3 of Fig. 3c). On the other hand, a portion of *Sargassum* near the southern boundary of box 2 has been transported southeastward by the LC to the Straits of Florida. The distributions of these surface currents and eddies, as well as the changes of *Sargassum* biomass density can be clearly visualized in an animation provided in the Supporting Information. Note that the southeastward currents on the West Florida Shelf and the currents associated with the two anticyclonic eddies in box 2 of Figs. 3c–3d had speeds of ~20–30 cm/s. In addition to the influence of ocean currents and eddies, the changes of wind direction from easterly to westerly or southwesterly (Le Hénaff and Kourafalou, 2016) may also have contributed to the eastward transport of *Sargassum*. A time series analysis was conducted to further understand the eastward transport of *Sargassum* within the GoM. Specifically, the time series of *Sargassum* biomass density over boxes 1–3 from May 16 to July 3, 2014, was derived from weekly running mean *Sargassum* areal density maps, and the results are presented in the inset figure of Fig. 3d. It is clear that box 1 was characterized by decreasing *Sargassum* biomass density, while box 2 was characterized by increasing biomass density until June 25 (annotated with a black vertical line in the inset figure), after which *Sargassum* biomass density decreased gradually. Regarding box 3, *Sargassum* biomass density increased sharply from June 16 to June 28. These results clearly demonstrate the eastward transport of *Sargassum* from west to east over the northern GoM.

The second category has not been described before in the refereed literature. In this pathway, *Sargassum* in the GoM has a remote origin in the tropical Atlantic Ocean where the Great Atlantic *Sargassum* Belt (GASB) forms nearly every spring–summer since 2011 (Gower et al., 2013; Wang et al., 2019; Gower and King, 2020). Specifically, large amounts of *Sargassum* were first observed in the tropical Atlantic Ocean during early spring, which were then transported to the Caribbean Sea via dominant ocean currents and eddies (Andrade-Canto et al., 2022), and eventually to the GoM from the Caribbean Sea. A similar transport mechanism was reported for satellite-tracked drifters launched in the eastern Caribbean Sea (Richardson, 2005) and the central Atlantic Ocean (Franks et al., 2016; Van Sebille et al., 2021; Drouin et al., 2022). Fig. 4 clearly shows that *Sargassum* in the northwestern Caribbean Sea is transported into the GoM by surface currents.

Upon entering the GoM, *Sargassum* can reach the central, western, northern, and southeastern GoM, as well as the Straits of Florida and even the east coast of Florida, all driven by ocean currents and eddies (as schematically shown in Fig. 2b). The LCS and eddies exhibit complicated spatial patterns within the GoM and the pattern evolution has variability on different time scales (e.g., Leben, 2005; Schmitz, 2005; Liu et al., 2016). The individual panels in Fig. 4 illustrate how the different transport pathways evolved in time, all controlled by the LCS, wind-driven ocean currents on the Campeche Bank, ocean currents in the northern/central GoM, and relevant eddies. These include the northward transport (Figs. 4a–4c), eastward transport (Figs. 4d–4f), and westward transport (Figs. 4g–4x).

The northward transport of *Sargassum* is illustrated in Figs. 4a–4c (corresponds to pathway #1 in Fig. 2b), where the positions of *Sargassum* at ~24, 26, and 28^{o}N correspond exactly to the three typical stages of the LC extension, including the “port-to-port”, “averagely extended”, and “fully extended” stages (shown as yellow, white, and green curves with arrows in Fig. 1a, respectively; Leben, 2005).

The eastward transport of *Sargassum* is shown in Figs. 4d–4f (corresponds to pathway #2 in Fig. 2b). During May 22–28, 2018, *Sargassum* appeared in the western branch of the LC. Four days later, *Sargassum* appeared in the eastern branch of the LC, and then was transported to the Straits of Florida during May 30–June 5, which finally reached the north Atlantic Ocean along the east coast of Florida.

The westward transport of *Sargassum* is more complex (Figs. 4g–4x), which can be characterized by the following six mechanisms:

(1) Westward transport of the wind-driven ocean currents on the Campeche Bank (pathway #3 in Fig. 2b and Figs. 4g–4i)
(2) Westward transport of the wind-driven ocean currents on the Campeche Bank and eddies (e.g., LC Eddies or LCEs; pathway #4 in Fig. 2b and Figs. 4j–4l, 5d–5e)
(3) Westward propagation of eddies (e.g., LCEs; pathway #5 in Fig. 2b and Figs. 4m–4o, 5d–5e)
(4) Relaying of eddies (pathway #6 in Fig. 2b and Figs. 4p–4r)
(5) Westward extension of the LCS (pathway #7 in Fig. 2b and Figs. 4s–4u)
(6) Westward transport of the westward currents with/without currents associated with eddies in the northern/central GoM (pathway #8 in Fig. 2b and Figs. 4v–4x)

As illustrated in Figs. 4g–4i, once *Sargassum* enters the GoM from the northwestern Caribbean Sea through the Yucatan Channel, the westward transport of the wind-driven ocean currents on the Campeche Bank (with schematic diagram shown in Figs. 1a and 2b) can bring *Sargassum* from the east to the west directly. On the other hand, if *Sargassum* encounters eddies (e.g., LCEs) during its westward transport driven by the wind-driven ocean currents on the Campeche Bank, the eddies can further

transport *Sargassum* westward (Figs. 4j–4l and 5d–5e). The third mechanism explaining the westward movement of *Sargassum* is shown in Figs. 4m–4r and 5d–5e. Specifically, the westward propagation of eddies (e.g., LCEs; annotated with white circles in Figs. 4m–4o and 5d–5e) allowed the westward transport of *Sargassum*, where *Sargassum* was mostly on the eddy edge rather than in the eddy center. Likewise, the relaying between eddies (e.g., LCEs) can allow *Sargassum* to be transported both westward and northward, as is clearly shown in Figs. 4p–4r and an animation provided in the Supporting Information.

After getting to the northern/northwestern edge of the LCS, the westward transport of *Sargassum* can be achieved through the westward extension of the LCS. As shown in Figs. 4s–4u, during August 5–11, 2021, *Sargassum* appeared on the western edge of the LCE at ~90ºW, and then reached ~92ºW after two weeks (Fig. 4u). The direct westward extension of the LCS within the two weeks facilitated the westward transport of *Sargassum*. Additionally, the westward transport of the westward currents with/without currents associated with eddies in the northern/central GoM can also transport *Sargassum* westward. According to Fig. 4v, the westward currents (annotated with white arrows in Figs. 4v–4x) moved *Sargassum* from the LCS to ~90ºW in mid-April 2022. These currents were the northern part of a cyclonic eddy and the southern part of an anticyclonic eddy (see clear pictures in an animation provided in the Supporting Information). In around one week, the cyclonic eddy entrained more *Sargassum* and lots of *Sargassum* was transported onto the Louisiana–Texas Shelf (Fig. 4w), and then *Sargassum* was transported further westward under the influence of the westward coastal currents (annotated with yellow arrows in Figs. 4v–4x) on the Louisiana–Texas Shelf in late April 2022 (Fig. 4x).

The durations (number of days) of the aforementioned transport mechanisms of *Sargassum* of Caribbean origin are summarized in Table 1 for the years after 2013, during which apparent transport pathways of

large amounts of *Sargassum* in the GoM have been observed in most years. It was found that each of the *Sargassum* transport mechanisms exhibited strong interannual variability, and that most of them lasted longer in major *Sargassum* years (e.g., 2018, 2019, 2021, and 2022) than in other years. In addition, among the six mechanisms of westward transport of *Sargassum*, the mechanisms involving the westward transport of the wind-driven ocean currents on the Campeche Bank with/without eddies, westward propagation of eddies, and the westward extension of the LCS play a more important role in the westward transport of GoM *Sargassum* compared to the other two (i.e., relaying of eddies; westward transport of the westward currents with/without currents associated with eddies in the northern/central GoM). It is worth mentioning that *Sargassum* transport mechanisms falling under the second category (remote origin in the tropical Atlantic Ocean) may occur concurrently. For instance, during the northward intrusion of the LC, *Sargassum* coming from the Caribbean Sea can be transported both northward and eastward by the LC in the GoM. In addition, a transition from one mechanism to another may occur gradually as the dynamic LCS evolves in time. Similarly, the transport of GoM *Sargassum* under the second category may also occur concurrently with the transport of *Sargassum* under the first category (i.e., local origin in the northwestern GoM).

The image sequences above clearly revealed the transport pathways of the observed large amounts of *Sargassum* in the GoM and the effects of the LCS on the *Sargassum* transport. Indeed, the LCS not only plays a key role in the northward, westward, and eastward transport of *Sargassum*, but can also regulate the spatial distribution patterns of *Sargassum*. On the other hand, even for the same physical mechanism of *Sargassum* transport (via the LCS) as shown above, the inter-annual variability of the LCS can lead to different *Sargassum* distribution patterns. For example, when the main axis of the LCS had a northward penetration at ~28^{o}N (Figs. 5a–5c), the spatial patterns of the LCS differed substantially in three different years (i.e., 2014, 2015, and 2021), as did the corresponding distribution patterns of *Sargassum*. A similar case can occur even within the same year (e.g., 2015), as demonstrated in Figs.

5d–5f. During the period of late July–late August 2015, *Sargassum* was transported westward by the westward movement of a LCE (white circles in Figs. 5d–5f) and the westward transport of the wind-driven ocean currents on the Campeche Bank (white ellipses in Figs. 5d–5f). The LCE-transported *Sargassum* decreased over time, while *Sargassum* transported by the wind-driven ocean currents first increased and then decreased. Such changes in *Sargassum* amount over time are also observed in Fig. 3. Specifically, during May 10–16, 2014, the stationary cyclonic eddy (yellow circle in Fig. 3) in the Bay of Campeche was virtually free of *Sargassum* (Fig. 3a). After two weeks, the *Sargassum* amount increased sharply (Fig. 3b), and then declined gradually starting from June 5th (Figs. 3c & 3d).

Another example is when the main axis of the LCS had a northward position at ~26^{o}N, where it can also significantly affect the spatial distribution patterns of *Sargassum* in different years (i.e., 2017, 2018, 2019; Figs. 5g–5i) and in the same year (i.e., 2018; Figs. 5j–5l). For the former cases, in both 2018 and 2019, more *Sargassum* was found than in 2017 in the northern part of the LCS (within the well-developed but still undetached LCE), when direct transport of *Sargassum* from the northwestern Caribbean Sea to the Straits of Florida also occurred (see the white curves with arrows in Figs. 5h & 5i). For the latter cases, between early June and late July of 2018, different locations/shapes of the LC and the undetached LCE led to different *Sargassum* transport and distribution patterns. During June 18–24 (Fig. 5k), the undetached LCE was oriented in the northwest–southeast direction, while it changed to the west–east direction during July 15–21 (Fig. 5l) when the LC penetrated further north (at ~24^{o}N). The distribution patterns of *Sargassum* closely followed these circulation patterns, which are dramatically different from those during June 7–13 (Fig. 5j).

In general, ocean surface currents and eddies in the GoM have strongly influenced the transport and spatial distribution patterns of *Sargassum*. In the adjacent Straits of Florida, where cyclonic eddy activity

is intense (Kourafalou and Kang, 2012; Zhang et al., 2019), ocean eddies also contribute to *Sargassum* transport. As shown in Fig. 6, *Sargassum* entrained within a cyclonic eddy was transported eastward along the Florida Keys due to the eastward movement of the eddy.

4. Discussion

The observations above are based on the combined *Sargassum* and surface ocean current maps, with the *Sargassum* distribution patterns explained by physical transport mechanisms. Although local growth and mortality can also change *Sargassum* abundance and distribution without physical transport, local growth is unlikely to explain the temporal changes in specific locations in the cases examined above. For example, under typical conditions, *Sargassum* daily doubling rate was estimated to be ~0.03 (Wang et al., 2019). Then, in one week, local growth would lead to an increase of $(2^{(0.03x7)} - 1) = 16\%$, and in two weeks the increased amount would be 34%, not sufficient to explain the much higher changes at fixed locations between sequential weekly images. Therefore, although local growth or mortality cannot be ruled out due to lack of *in situ* data, their roles in determining the spatial distribution patterns of *Sargassum* are likely minor as compared to physical transport.

It should be noted that the growth rate of *Sargassum* varies over time, and the method (e.g., *in situ* and ex-situ culture systems vs satellite observations) used to calculate the growth rate can also influence the results. In this study, the selected daily *Sargassum* doubling rate (~0.03) is a mean growth rate, derived from satellite observations of *Sargassum* during *Sargassum* growing seasons (Wang et al., 2019), and it can be smaller than the growth rates derived from *in situ* and ex-situ culture systems (e.g., ~0.03–0.06 from Magaña-Gallegos et al., 2023). In addition, we note that in many previous studies of pelagic *Sargassum* (e.g., Johns et al., 2020; Marsh et al., 2021), 1% windage (i.e., 1% of the 10 m winds; direct momentum transfer from the winds to floating materials) has been added to surface current velocity field

to achieve better understanding of *Sargassum* transport and prediction. Here, 1% windage for the GoM (equivalent to ~0.01–0.06 m/s; Zhang and Hu, 2021) is negligible compared to the strong ocean current field of the GoM (e.g., >0.5 m/s for the LC/FC system and LCEs, Liu et al., 2016 and Zhang et al., 2023; ~0.3–0.35 m/s for the ocean currents on the Campeche Bank, Lilly and Pérez-Brunius 20221), therefore, windage effects were not considered in this study.

Similar to ocean currents, Stokes drift (residual transport due to ocean waves) can also contribute to the transport of drifting materials, particularly in shallow, nearshore waters (e.g., Monismith and Fong, 2004; Röhrs et al., 2012; Hunter et al. 2022), which induces a displacement of materials parallel to the direction of wave propagation (Jouanno et al., 2021). This mechanism allows *Sargassum* to migrate and possibly accumulate in shallow waters along the coasts. The effects due to Stokes drift are not considered in this paper because 1) the focus of this study is on the transport of large amounts of pelagic *Sargassum* in the open GoM rather than in shallow nearshore waters where the influence of ocean waves is more important, and 2) in the open GoM surface current velocities are generally ~8–10 times larger than Stokes drift velocities (Bosi et al., 2021). This omission is consistent with previous studies focusing on the simulation and prediction of *Sargassum* transport in the tropical and subtropical North Atlantic (e.g., Brooks et al., 2018; Putman et al., 2018; Wang et al., 2019; Marsh et al., 2021). Nevertheless, future studies on *Sargassum* transport in shallow nearshore waters should consider the Stokes drift effects.

The findings above have significant implications on *Sargassum* forecasts for sensitive coastal habitats in Florida, where recurrent beaching events have been reported in the Florida Keys and along the east coast of Florida (e.g., Miami Beach and Palm Beach; Trinanes et al., 2021; Zhang S. et al., 2022). For example, how long will it take to transport *Sargassum* from the northwestern Caribbean Sea, or from the northern edge of the LCS, to the Florida Keys and the east coast of Florida? Figs. 7a–7i show an example

of continuous transport of *Sargassum* from the northwestern Caribbean Sea to the Florida Keys and east coast of Florida. From this image sequence, *Sargassum* reached the northern edge of the LC during May 24–30, 2018 (Fig. 7c) and was then transported to the Florida Keys in about 5 days (Figs. 7c–7f). After about 3 more days, *Sargassum* reached the east coast of Florida near Miami (Fig. 7h). These results can be explained by the mean velocity of the LC/FC system (~1.2–1.6 m/s, Zhang Y. et al., 2022).

The transport can also be revealed through a lag analysis of time series of *Sargassum* wet biomass (as shown in Fig. 7j). For the period January 2013–February 2022, the two time series of the northwestern Caribbean Sea (blue color in Fig. 7j) and around the southeast coast of Florida (red color in Fig. 7j) suggest a one-month lag between the two, especially in the summer months of major *Sargassum* years of 2015, 2017, 2018, and 2020. The two exceptional years are 2019 and 2021, when *Sargassum* was transported to south Florida directly from the tropical Atlantic Ocean via the North Equatorial Current and the Antilles Current (Drouin et al., 2022), as observed from the SaWS (https://optics.marine.usf.edu/projects/saws.html). Another exception occurred in 2014, when *Sargassum* in the GoM appeared to have a local origin (as shown in Fig. 3). In all cases, the *Sargassum* amount in the latter region is not necessarily proportional to that in the former region, clearly indicating the complexity of *Sargassum* transport and growth. Note that the one-month lag described here is different from the number of days when the eastward transport of *Sargassum* was observed during a year (third column of Table 1): the former is directly relevant to the behavior and velocity of the Loop Current/Florida Current system, while the latter indicates how often such an eastward transport occurs.

Finally, our findings on the *Sargassum* transport in the GoM were made possible not only by the availability of advanced satellite-based *Sargassum* products, but also by the full use of ocean surface current products derived from multiple altimeters. The method used in this study can be extended to

other relevant topics, such as marine debris and spilled oil transport (e.g., Liu et al., 2011; Kourafalou and Androulidakis, 2013; Jolliff et al., 2014; Abascal et al., 2015; Weisberg et al., 2011, 2017). Indeed, the transport mechanisms of GoM *Sargassum* introduced in this study represent the dominant mechanisms responsible for the transport of large amounts of *Sargassum* in the GoM, which were derived from the combined maps of *Sargassum* areal density (0.1° × 0.1°) and altimetry-based surface geostrophic currents (0.25° × 0.25°). The transport mechanisms of GoM *Sargassum* at smaller scale may have been overlooked here, and the *Sargassum* transport mechanisms over the coastal areas (e.g., the West Florida Shelf and Louisiana–Texas Shelf) may have not be fully revealed due to the deficiencies in current satellite altimetry products. However, these limitations may be overcome with the availability of novel surface current products at higher spatial resolution from more advanced satellite altimetry missions (e.g., Surface Water and Ocean Topography or SWOT; https://swot.jpl.nasa.gov/). Moreover, in addition to surface currents, reliable data on local winds, waves, and tides are also essential in interpreting *Sargassum* beaching in nearshore coastal waters. In such environments, the processes elucidating how *Sargassum* detaches from major surface currents remain unknown and therefore should be investigated in future research.

5. Conclusions

Based on satellite observations of *Sargassum* areal density and ocean surface currents, we have shown that large amounts of *Sargassum* in the GoM can either originate from the northwestern GoM or be a result of physical transport from the northwestern Caribbean Sea, each having their specific transport pathways that influence the spatial distribution patterns of this brown seaweed. The LCS and associated eddies were found to play a key role in the *Sargassum* transport within the GoM. Time series analysis also revealed that *Sargassum* along the southeast coast of Florida may lag *Sargassum* in the northwestern

Caribbean Sea by about one month in most years with major *Sargassum* blooms, all under the influence of the Great Atlantic *Sargassum* Belt.

Notations

FC	Florida Current
GASB	Great Atlantic Sargassum Belt
GoM	Gulf of Mexico
LC	Loop Current
LCE	Loop Current Eddies
LCS	Loop Current System
MERIS	Medium Resolution Imaging Spectrometer
MODIS	Moderate Resolution Imaging Spectroradiometer
OLCI	Ocean and Land Colour Imager
SaWS	*Sargassum* Watch System

Declaration of Competing Interest

The authors declare that they have no known competing financial interests or personal relationships that could have appeared to influence the work reported in this paper.

Data Availability Statement

The data products used in this study are publicly available. Weekly *Sargassum* areal density data products were generated and distributed through the *Sargassum* Watch System (SaWS, https://optics.marine.usf.edu/projects/saws.html) by the Optical Oceanography Laboratory at the

University of South Florida. The altimetry data products were obtained from the Copernicus Marine Environment Monitoring Service (https://resources.marine.copernicus.eu/products).

Acknowledgments

This work was supported by the NASA student fellowship program "Future Investigators in NASA Earth and Space Science and Technology" (FINESST, 80NSSC19K1358), NASA Ocean Biology and Biogeochemistry program (80NSSC20M0264), NASA Biodiversity and Ecological Forecasting program (80NSSC21K0422), NOAA NCCOS MERHAB program (NA23NOS4780291), EPA South Florida program (02D42923), National Academy of Sciences Gulf Research Program (SCON-10000542), NOAA RESTORE Science Program (NA17NOS4510099), National Science Foundation (OCE-1840381), National Institute of Environmental Health Sciences (1P01ES028938), and the Isham Family Charitable Fund. We thank the two anonymous reviewers for their constructive comments and suggestions to improve the presentation of this work.

Supporting Information

The animation showing the eastward transport of Sargassum from the northwestern GoM to the eastern GoM can be accessed at:
https://optics.marine.usf.edu/projects/GoM_Sargassum_transport/NW_GoM_Sargassum_eastward_transport.html

The animation showing the westward transport of Sargassum controlled by mechanism 4 (i.e., relaying of ocean eddies) and mechanism 6 (i.e., westward transport of the westward ocean currents with/ without currents associated with eddies in the northern/central GoM) can be accessed at:https://optics.marine.usf.edu/projects/GoM_Sargassum_transport/GoM_Sargassum_westward_transport_animation.html

References

Abascal, A.J., Castanedo, S., Minguez, R., Medina, R., Liu, Y., and Weisberg, R.H., 2015. Stochastic Lagrangian trajectory modeling of surface drifters deployed during the Deepwater Horizon oil spill. In *Proc. 38th AMOP Tech. Seminar Env. Contamination & Response, Env. & Climate Change Canada*, Ottawa, ON, PP. 71–99.

Alvera-Azcárate, A., Barth, A., and Weisberg, R.H., 2009. The surface circulation of the Caribbean Sea and the Gulf of Mexico as inferred from satellite altimetry. *Journal of Physical Oceanography*, 39(3), pp.640-657. https://doi.org/10.1175/2008JPO3765.1.

Amador-Castro, F., García-Cayuela, T., Alper, H.S., Rodriguez-Martinez, V. and Carrillo-Nieves, D., 2021. Valorization of pelagic *Sargassum* biomass into sustainable applications: Current trends and challenges. *Journal of Environmental Management*, 283, p.112013. https://doi.org/10.1016/j.jenvman.2021.112013.

Andrade-Canto, F., Beron-Vera, F.J., Goni, G.J., Karrasch, D., Olascoaga, M.J., and Triñanes, J., 2022. Carriers of *Sargassum* and mechanism for coastal inundation in the Caribbean Sea. *Physics of Fluids*, 34(1), p.016602. https://doi.org/10.1063/5.0079055.

Brooks, M.T., Coles, V.J., Hood, R.R., and Gower, J.F., 2018. Factors controlling the seasonal distribution of pelagic *Sargassum*. *Marine Ecology Progress Series*, 599, pp.1-18. https://doi.org/10.3354/meps12646.

Bosi, S., Broström, G., and Roquet, F., 2021. The role of Stokes drift in the dispersal of North Atlantic surface marine debris. *Frontiers in Marine Science*, 8, p.697430. https://doi.org/10.3389/fmars.2021.697430.

447 Casazza T.L., and Ross S.W., 2008. Fishes associated with pelagic *Sargassum* and open water lacking
448 *Sargassum* in the Gulf Stream of North Carolina. *Fishery Bulletin*, 106(4):348–363.

449 Chen, Y., 2017. Fish resources of the Gulf of Mexico. In C. Ward (Ed.), *Habitats and biota of the Gulf*
450 *of Mexico: Before the Deepwater Horizon oil spill*. Springer. https://doi.org/10.1007/978-1-4939-
451 3456-0_1.

452 Doyle, E. and Franks, J., 2015. *Sargassum* fact sheet. Gulf and Caribbean Fisheries Institute (4 pp.).

453 Drouin, K.L., Lozier, M.S., Beron-Vera, F.J., Miron, P. and Olascoaga, M.J., 2022. Surface pathways
454 connecting the South and North Atlantic oceans. *Geophysical Research Letters*, 49,
455 e2021GL096646. https://doi.org/10.1029/2021GL096646.

456 Elliott, B.A., 1982. Anticyclonic rings in the Gulf of Mexico. *Journal of Physical Oceanography*, 12(11),
457 pp.1292-1309. DOI: https://doi.org/10.1175/1520-0485(1982)012<1292:ARITGO>2.0.CO;2.

458 Felder, D.L., Camp, D.K. and Tunnel, W., Jr., 2009. An introduction to Gulf of Mexico biodiversity
459 assessment. In D.L. Felder and D.K. Camp (Eds.), *Gulf of Mexico origin, waters, and biota*, Volume
460 1, Biodiversity. Texas A&M University Press.

461 Franks, J.S., Johnson, D.R. and Ko, D.S., 2016. Pelagic *Sargassum* in the tropical North Atlantic. *Gulf*
462 *and Caribbean Research*, 27(1), pp.SC6-SC11. DOI: https://doi.org/10.18785/gcr.2701.08.

463 Gower, J., Hu, C., Borstad, G., & King, S., 2006. Ocean color satellites show extensive lines of floating
464 *Sargassum* in the Gulf of Mexico. *IEEE Transactions on Geoscience and Remote Sensing*, 44, 3619–
465 3625. DOI: 10.1109/TGRS.2006.882258.

Gower, J., & King, S., 2011. Distribution of floating *Sargassum* in the Gulf of Mexico and the Atlantic Ocean mapped using MERIS. *International Journal of Remote Sensing*, 32, 1917–1929. DOI: 10.1080/01431161003639660.

Gower, J., Young, E., and King, S., 2013. Satellite images suggest a new *Sargassum* source region in 2011. *Remote Sensing Letters*, 4(8), pp.764-773. DOI: 10.1080/2150704X.2013.796433.

Gower, J., and King, S., 2019. Seaweed, seaweed everywhere. *Science*, 365(6448), pp.27-27. DOI: 10.1126/science.aay0989.

Gower, J., and King, S., 2020. The distribution of pelagic *Sargassum* observed with OLCI. *International Journal of Remote Sensing*, 41(15), pp.5669-5679. DOI: 10.1080/01431161.2019.1658240.

Hamilton, P., Fargion, G.S., and Biggs, D.C., 1999. Loop Current eddy paths in the western Gulf of Mexico. *Journal of physical Oceanography*, 29(6), pp.1180-1207. https://doi.org/10.1175/1520-0485(1999)029<1180:LCEPIT>2.0.CO;2.

Hu, C., J. Cannizzaro, K. L.Carder, F. E. Muller-Karger, and R. Hardy (2010). Remote detection of Trichodesmium blooms in optically complex coastal waters: Examples with MODIS full-spectral data. Remote Sens. Environ., 114:2048-2058

Hu, C., Hardy, R., Ruder, E., Geggel, A., Feng, L., Powers, S., Hernandez, F., Graettinger, G., Bodnar, J., and McDonald, T., 2016a. *Sargassum* coverage in the northeastern Gulf of Mexico during 2010 from Landsat and airborne observations: Implications for the Deepwater Horizon oil spill impact assessment. *Marine Pollution Bulletin*, 107(1), pp.15-21. https://doi.org/10.1016/j.marpolbul.2016.04.045.

Hu, C., Murch, B., Barnes, B.B., Wang, M., Maréchal, J.P., Franks, J., Johnson, D., Lapointe, B.E., Goodwin, D.S., Schell, J.M., and Siuda, A.N.S., 2016b. *Sargassum* watch warns of incoming seaweed. *Eos*. 97:10–15. https://doi.org/10.1029/2016EO058355.

Hu, C., Wang, M., Lapointe, B.E., Brewton, R.A., and Hernandez, F.J., 2021. On the Atlantic pelagic *Sargassum*'s role in carbon fixation and sequestration. *Science of the Total Environment*, 781, p.146801. https://doi.org/10.1016/j.scitotenv.2021.146801.

Hunter, E.J., Fuchs, H.L., Wilkin, J.L., Gerbi, G.P., Chant, R.J., and Garwood, J.C., 2022. ROMSPath v1. 0: offline particle tracking for the Regional Ocean Modeling System (ROMS). *Geoscientific Model Development*, 15(11), pp.4297-4311. https://doi.org/10.5194/gmd-15-4297-2022.

Johns, E.M., Lumpkin, R., Putman, N.F., Smith, R.H., Muller-Karger, F.E., Rueda-Roa, D.T., Hu, C., Wang, M., Brooks, M.T., Gramer, L.J. and Werner, F.E., 2020. The establishment of a pelagic *Sargassum* population in the tropical Atlantic: Biological consequences of a basin-scale long distance dispersal event. *Progress in Oceanography*, 182, p.102269. https://doi.org/10.1016/j.pocean.2020.102269.

Jolliff, J.K., Smith, T.A., Ladner, S. and Arnone, R.A., 2014. Simulating surface oil transport during the Deepwater Horizon oil spill: Experiments with the BioCast system. *Ocean Modelling*, 75, pp.84-99. https://doi.org/10.1016/j.ocemod.2014.01.004.

Jouanno, J., Benshila, R., Berline, L., Soulié, A., Radenac, M.H., Morvan, G., Diaz, F., Sheinbaum, J., Chevalier, C., Thibaut, T., and Changeux, T., 2021. A NEMO-based model of *Sargassum* distribution in the tropical Atlantic: description of the model and sensitivity analysis (NEMO-Sarg1.0). *Geoscientific Model Development*, 14(6), pp.4069-4086. https://doi.org/10.5194/gmd-14-4069-2021.

508 Kourafalou, V. H., & Kang, H., 2012. Florida Current meandering and evolution of cyclonic eddies
509 along the Florida Keys Reef Tract: Are they interconnected? *Journal of Geophysical Research:*
510 *Oceans*, 117, C05028. https://doi.org/10.1029/2011JC007383.

511 Kourafalou, V. H., and Androulidakis, Y. S., 2013, Influence of Mississippi River induced circulation
512 on the Deepwater Horizon oil spill transport. *Journal of Geophysical Research Oceans*, 118, 3823–
513 3842, doi:10.1002/jgrc.20272.

514 Lapointe, B. E., R. A. Brewton, L. W. Herren, M. Wang, C. Hu, D. J. McGillicuddy, Jr., S. Lindell, F.
515 J. Hernandez, and P. L. Morton (2021). Nutrient content and stoichiometry of pelagic Sargassum
516 reflects increasing nitrogen availability in the Atlantic Basin. Nature Communications. 12:3060,
517 https://doi.org/10.1038/s41467-021-23135-7

518 Leben, R.R., 2005. Altimeter-Derived Loop Current Metrics. In *Circulation in the Gulf of Mexico:*
519 *Observations and Models* (eds W. Sturges and A. Lugo‐ Fernandez).
520 https://doi.org/10.1029/161GM15.

521 Le Hénaff, M., and Kourafalou, V.H., 2016. Mississippi waters reaching South Florida reefs under no
522 flood conditions: synthesis of observing and modeling system findings. *Ocean Dynamics*, 66(3),
523 pp.435-459. https://doi.org/10.1007/s10236-016-0932-4.

524 Lilly, J.M. and Pérez-Brunius, P., 2021. A gridded surface current product for the Gulf of Mexico from
525 consolidated drifter measurements. *Earth System Science Data*, 13(2), pp.645-669.
526 https://doi.org/10.5194/essd-13-645-2021.

527 Liu, Y., Weisberg, R.H., Hu, C., and Zheng, L., 2011. Tracking the Deepwater Horizon oil spill: A
528 modeling perspective. *Eos, Transactions American Geophysical Union*, 92(6), pp.45-46.
529 doi:10.1029/2011EO060001.

Liu, Y., Weisberg, R.H., Vignudelli, S., and Mitchum, G.T., 2014. Evaluation of altimetry-derived surface current products using Lagrangian drifter trajectories in the eastern Gulf of Mexico. *Journal of Geophysical Research Oceans*, 119, 2827-2842, doi:10.1002/2013JC009710.

Liu, Y., Weisberg, R.H., Vignudelli, S., and Mitchum, G.T., 2016. Patterns of the loop current system and regions of sea surface height variability in the eastern Gulf of Mexico revealed by the self-organizing maps. *Journal of Geophysical Research: Oceans*, 121(4), pp.2347-2366, doi:10.1002/2015JC011493.

Magaña-Gallegos, E., García-Sánchez, M., Graham, C., Olivos-Ortiz, A., Siuda, A.N. and van Tussenbroek, B.I., 2023. Growth rates of pelagic *Sargassum* species in the Mexican Caribbean. *Aquatic Botany*, 185, p.103614. https://doi.org/10.1016/j.aquabot.2022.103614.

Marsh, R., Addo, K.A., Jayson-Quashigah, P.N., Oxenford, H.A., Maxam, A., Anderson, R., Skliris, N., Dash, J., and Tompkins, E.L., 2021. Seasonal predictions of holopelagic *Sargassum* across the tropical Atlantic accounting for uncertainty in drivers and processes: the SARTRAC ensemble forecast system. *Frontiers in Marine Science*, 8, p.722524. https://doi.org/10.3389/fmars.2021.722524.

Martin, L.M., Taylor, M., Huston, G., Goodwin, D.S., Schell, J.M. and Siuda, A.N., 2021. Pelagic *Sargassum* morphotypes support different rafting motile epifauna communities. *Marine Biology*, 168, pp.1-17. https://doi.org/10.1007/s00227-021-03910-2.

McGillicuddy, D. J. Jr., P. L. Morton, R. A. Brewton, C. Hu, T. B. Kelly, A. R. Solow, and B. E. Lapointe (2023). Nutrient and arsenic biogeochemistry of Sargassum in the western Atlantic. Nature Communications. 14:6205, https://doi.org/10.1038/s41467-023-41904-4.

551 Milledge, J.J., Nielsen, B.V., and Bailey, D., 2016. High-value products from macroalgae: the potential
552 uses of the invasive brown seaweed, *Sargassum* muticum. *Reviews in Environmental Science and*
553 *Bio/Technology*, 15(1), pp.67-88. https://doi.org/10.1007/s11157-015-9381-7.

554 Monismith, S.G. and Fong, D.A., 2004. A note on the potential transport of scalars and organisms by
555 surface waves. *Limnology and Oceanography*, 49(4), pp.1214-1217.
556 https://doi.org/10.4319/lo.2004.49.4.1214.

557 Orozco-González, J.G., Amador-Castro, F., Gordillo-Sierra, A.R., García-Cayuela, T., Alper, H.S. and
558 Carrillo-Nieves, D., 2022. Opportunities surrounding the use of *Sargassum* biomass as precursor of
559 biogas, bioethanol, and biodiesel production. *Frontiers in Marine Science*, 8, p.791054.
560 https://doi.org/10.3389/fmars.2021.791054.

561 Putman, N.F., Goni, G.J., Gramer, L.J., Hu, C., Johns, E.M., Trinanes, J., and Wang, M., 2018.
562 Simulating transport pathways of pelagic *Sargassum* from the Equatorial Atlantic into the Caribbean
563 Sea. *Progress in oceanography*, 165, pp.205-214. https://doi.org/10.1016/j.pocean.2018.06.009.

564 Qi, L., C. Hu, K. MIkelsons, M. Wang, V. Lance, S. Sun, B. B. Barnes, J. Zhao, and D. V. der Zande
565 (2020). In search of floating algae and other organisms in global oceans and lakes. Remote Sens.
566 Environ., 239, 111659, https://doi.org/10.1016/j.rse.2020.111659.

567 Richardson, P.L., 2005. Caribbean Current and eddies as observed by surface drifters. *Deep Sea*
568 *Research Part II: Topical Studies in Oceanography*, 52(3-4), pp.429-463.
569 https://doi.org/10.1016/j.dsr2.2004.11.001.

570 Röhrs, J., Christensen, K.H., Hole, L.R., Broström, G., Drivdal, M., and Sundby, S., 2012. Observation-
571 based evaluation of surface wave effects on currents and trajectory forecasts. *Ocean Dynamics*, 62,
572 pp.1519-1533. https://doi.org/10.1007/s10236-012-0576-y.

573 Sanchez-Rubio, G., Perry, H., Franks, J.S. and Johnson, D.R., 2018. Occurrence of pelagic *Sargassum*
574 in waters of the U.S. Gulf of Mexico in response to weather-related hydrographic regimes associated
575 with decadal and interannual variability in global climate. *Fishery Bulletin*, 116(1), p93-106. DOI:
576 10.7755/FB.116.1.10.

577 Schmitz, W.J., Jr., 2005. Cyclones and Westward Propagation in the Shedding of Anticyclonic Rings
578 from the Loop Current. In *Circulation in the Gulf of Mexico: Observations and Models* (eds W.
579 Sturges and A. Lugo‐ Fernandez). https://doi.org/10.1029/161GM18.

580 Siuda, A.N., Schell, J.M. and Goodwin, D.S., 2016. Unprecedented proliferation of novel pelagic
581 *Sargassum* form has implications for ecosystem function and regional diversity in the Caribbean.
582 American Geophysical Union, Ocean Sciences Meeting 2016, pp.ME14E-0682.

583 Smetacek, V., and Zingone, A., 2013. Green and golden seaweed tides on the rise. *Nature*, 504(7478),
584 pp.84-88. https://doi.org/10.1038/nature12860.

585 Trinanes, J., Putman, N.F., Goni, G., Hu, C., and Wang, M., 2021. Monitoring pelagic *Sargassum*
586 inundation potential for coastal communities. *Journal of Operational Oceanography*, pp.1-12.
587 https://doi.org/10.1080/1755876X.2021.1902682.

588 Van Sebille, E., Zettler, E., Wienders, N., Amaral-Zettler, L., Elipot, S. and Lumpkin, R., 2021.
589 Dispersion of surface drifters in the Tropical Atlantic. *Frontiers in Marine Science*, 7, p.607426.
590 https://doi.org/10.3389/fmars.2020.607426.

591 Van Tussenbroek, B.I., Arana, H.A.H., Rodríguez-Martínez, R.E., Espinoza-Avalos, J., Canizales-Flores,
592 H.M., González-Godoy, C.E., Barba-Santos, M.G., Vega-Zepeda, A. and Collado-Vides, L., 2017.
593 Severe impacts of brown tides caused by *Sargassum* spp. on near-shore Caribbean seagrass

communities. *Marine pollution bulletin*, 122(1-2), pp.272-281. https://doi.org/10.1016/j.marpolbul.2017.06.057.

Vignudelli, S., Snaith, H.M., Lyard, F., Cipollini, P., Venuti, F., Birol, F., Bouffard, J., and Roblou, L., 2006. Satellite radar altimetry from open ocean to coasts: challenges and perspectives. *Remote Sensing of the Marine Environment*, 6406, pp.148-159. https://doi.org/10.1117/12.694024.

Wang, M., and Hu, C., 2016. Mapping and quantifying *Sargassum* distribution and coverage in the Central West Atlantic using MODIS observations. *Remote Sensing of Environment*, 183, pp.350-367. http://dx.doi.org/10.1016/j.rse.2016.04.019.

Wang, M., and Hu, C., 2017. Predicting *Sargassum* blooms in the Caribbean Sea from MODIS observations. *Geophysical Research Letters*, 44(7), pp.3265-3273. https://doi.org/10.1002/2017GL072932.

Wang, M., Hu, C., Cannizzaro, J., English, D., Han, X., Naar, D., Lapointe, B., Brewton, R., and Hernandez, F., 2018. Remote sensing of *Sargassum* biomass, nutrients, and pigments. *Geophysical Research Letters*, 45(22), pp.12-359. https://doi.org/10.1029/2018GL078858.

Wang, M., Hu, C., Barnes, B.B., Mitchum, G., Lapointe, B., and Montoya, J.P., 2019. The great Atlantic *Sargassum* belt. *Science*, 365(6448), pp.83-87. DOI: 10.1126/science.aaw7912.

Webster, R.K. and Linton, T., 2013. Development and implementation of *Sargassum* early advisory system (SEAS). *Shore & Beach*, 81(3), p.1.

Weisberg, R. H., Zheng, L., and Liu, Y., 2011. "Tracking subsurface oil in the aftermath of the Deepwater Horizon well blowout," in *Monitoring and Modeling the Deepwater Horizon Oil Spill: A Record-Breaking Enterprise. Geophys. Monogr. Ser*., Vol. 195, eds Y. Liu, A. MacFadyen, Z.-G.

615 Ji, and R. H. Weisberg (Washington, DC: The American Geophysical Union), 205–215. doi:
616 10.1029/2011GM001131.

617 Weisberg, R.H., Zheng, L., Liu, Y., Murawski, S., Hu, C., and Paul, J., 2016. Did Deepwater Horizon
618 hydrocarbons transit to the west Florida continental shelf? *Deep Sea Research Part II: Topical*
619 *Studies in Oceanography*, 129, pp.259-272. https://doi.org/10.1016/j.dsr2.2014.02.002.

620 Weisberg, R.H., Zheng, L., and Liu, Y., 2017. On the movement of Deepwater Horizon Oil to northern
621 Gulf beaches. *Ocean Modelling*, 111, pp.81-97. https://doi.org/10.1016/j.ocemod.2017.02.002.

622 Wells, R.J., and Rooker, J.R., 2004. Spatial and temporal patterns of habitat use by fishes associated
623 with *Sargassum* mats in the northwestern Gulf of Mexico. *Bulletin of Marine Science*, 74(1), pp.81-
624 99.

625 Witherington, B.; Hirama, S., and Hardy, R., 2012. Young sea turtles of the pelagic *Sargassum*-
626 dominated drift community: Habitat use, population density, and threats. *Marine Ecology Progress*
627 *Series*, 463, 1–22. DOI: 10.3354/meps09970.

628 Zavala-Hidalgo, J., Romero-Centeno, R., Mateos-Jasso, A., Morey, S. L., and Martínez-López, B., 2014.
629 The response of the Gulf of Mexico to wind and heat flux forcing: What has been learned in recent
630 years? *Atmósfera*, 27(3), 317–334. https://doi.org/10.1016/s0187-6236(14)71119-1.

631 Zhang, S., Hu, C., Barnes, B.B., and Harrison, T.N., 2022. Monitoring *Sargassum* Inundation on Beaches
632 and Nearshore Waters Using PlanetScope/Dove Observations. *IEEE Geoscience and Remote*
633 *Sensing Letters*, 19, pp.1-5. DOI: 10.1109/LGRS.2022.3148684.

634 Zhang, Y., Hu, C., Liu, Y., Weisberg, R. H., and Kourafalou, V. H., 2019. Submesoscale and mesoscale
635 eddies in the Florida straits: observations from satellite ocean color measurements. *Geophysical*
636 *Research Letters*, 46, 13262–13270. https://doi.org/10.1029/2019GL083999.

637 Zhang, Y., & Hu, C., 2021. Ocean temperature and color frontal zones in the Gulf of Mexico: Where,
638 when, and why. *Journal of Geophysical Research: Oceans*, 126, e2021JC017544.
639 https://doi.org/10.1029/2021JC017544.

640 Zhang, Y., Hu, C., Kourafalou, V.H., Liu, Y., McGillicuddy, D.J., Barnes, B.B., and Hummon, J.M.,
641 2022. Physical characteristics and evolution of a long-lasting mesoscale cyclonic eddy in the Straits
642 of Florida. *Frontiers in Marine Science*, 9, 779450. https://doi.org/10.3389/fmars.2022.779450.

643 Zhang, Y., Hu, C., Barnes, B. B., Liu, Y., Kourafalou, V. H., McGillicuddy, D. J., et al., 2023. Bio-
644 optical, physical, and chemical properties of a Loop Current Eddy in the Gulf of Mexico. *Journal*
645 *of Geophysical Research: Oceans*, 128, e2022JC018726. https://doi.org/10.1029/2022JC018726.

646 Zhu, Y., & Liang, X., 2020. Coupling of the surface and near-bottom currents in the Gulf of Mexico.
647 *Journal of Geophysical Research: Oceans*, 125, e2020JC016488.
648 https://doi.org/10.1029/2020JC016488.

649

650

651

652

653

654

655

656

657

Tables and captions

Table 1. Durations (number of days) of different transport pathways of *Sargassum* of Caribbean origin in the GoM, determined from "daily" *Sargassum* biomass density images (calculated as an average of the past seven days with the current day included) between January 2014 and June 2023. This analysis is focused on years after 2013, before which the *Sargassum* amount in the Caribbean Sea was minimal.

Mechanism / Year	Northward transport	Eastward transport	Westward transport (M-1)	Westward transport (M-2)	Westward transport (M-3)	Westward transport (M-4)	Westward transport (M-5)	Westward transport (M-6)
2014	127	73	53	0	40	0	41	0
2015	60	152	76	58	70	10	65	6
2016	0	0	0	0	0	0	0	0
2017	114	98	42	0	11	0	43	10
2018	159	196	152	68	98	10	87	8
2019	228	239	71	71	25	22	180	47
2020	68	75	67	51	23	9	27	0
2021	124	161	112	61	41	11	151	0
2022	172	197	143	84	93	41	170	25
2023	120	130	74	0	17	12	116	34

Figures and captions (*color is required for all figures in print*)

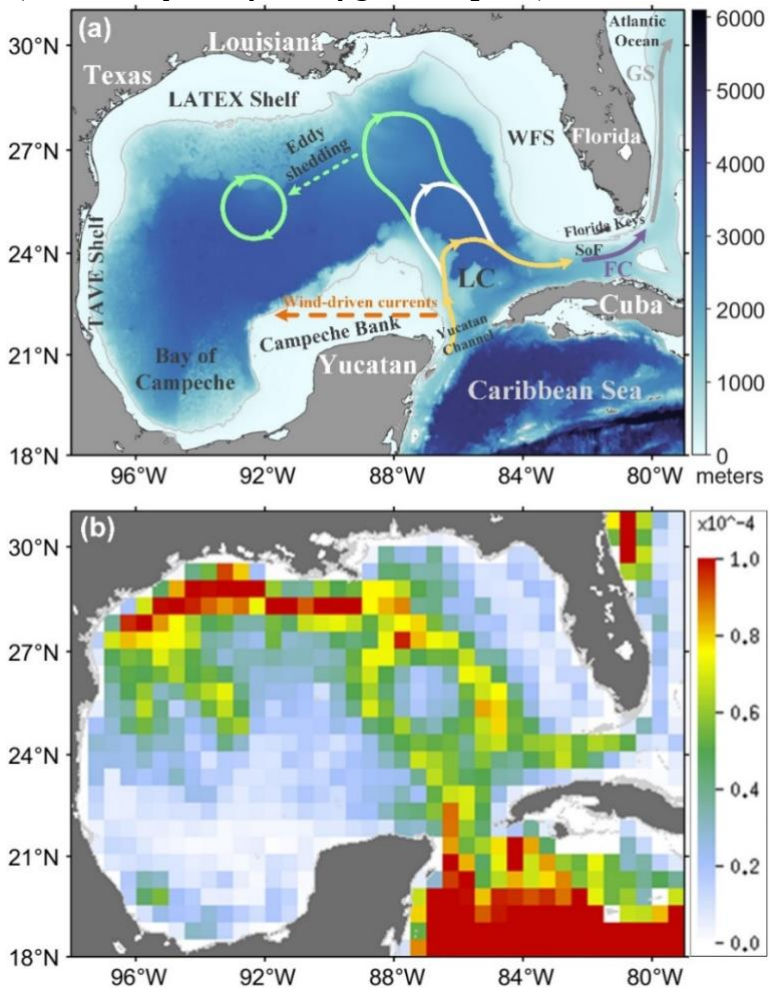

Figure 1. (a) Bathymetry of the Gulf of Mexico and the northwestern Caribbean Sea. The thin gray lines denote the 200 m isobath. Important geographic features are also noted: Yucatan Channel, Straits of Florida (SoF), Florida Keys, West Florida Shelf (WFS), Louisiana–Texas (LATEX) Shelf, Tamaulipas–Veracruz (TAVE) Shelf, Bay of Campeche, Campeche Bank, and the Atlantic Ocean. The Florida Current (FC) and Gulf Stream (GS) are indicated by thick purple and gray curves with arrows, respectively. The dashed orange line with an arrow on the Campeche Bank denotes the ocean currents driven by northeasterly or easterly winds throughout the year (e.g., Zavala-Hidalgo et al., 2014; Zhang and Hu, 2021). The yellow, white, and green curves with arrows individually denote the Loop Current (LC) extension in three different stages (i.e., "port-to-port", "averagely extended", and "fully extended"), during which it has a northward extension at ~24, 26, and 28°N, respectively (Leben, 2005). After extending northward from ~24°N to ~28°N, a large anticyclonic LC Eddy (LCE, green circle) may form and detach from the extended LC. Before its final separation from the LC, the LCE may re–attach to, and detach from the LC several times (Leben, 2005; Schmitz, 2005). After the separation from the LC, LCEs predominantly propagate westward at speeds of ~2–5 km/day (Elliott, 1982; Hamilton et al., 1999). (b) Distribution of mean *Sargassum* areal density during April–September of 2011–2020, with a grid size of 0.5°. Color codes denote fractional cover (e.g., 1×10^{-4} = 0.01%). Note that the weekly *Sargassum* areal density images used in this study have a grid size of 0.1°.

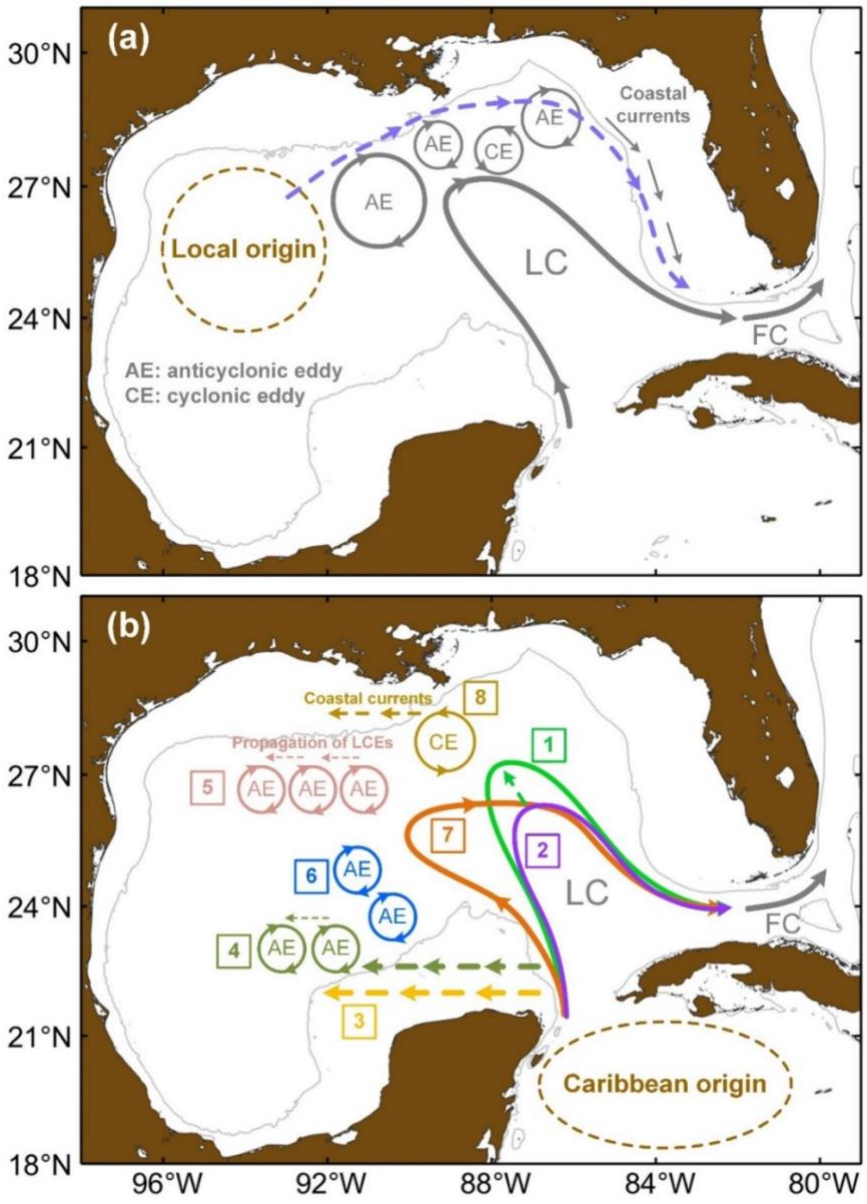

Figure 2. Schematic diagrams showing the major transport pathways of GoM *Sargassum* of (a) local origin and (b) Caribbean origin. The thin gray lines in each figure denote the 200 m isobath. LC and FC represent the Loop Current and Florida Current, respectively. The dashed blue curves with arrows in (a) indicate the eastward transport pathway of *Sargassum* of local origin, associated with ocean eddies in the northern GoM and the southeastward coastal currents on the West Florida Shelf. *Sargassum* transport pathways shown in (b) are listed as follows. 1: northward transport by the northward intrusion of the Loop Current extension; 2: eastward transport by the direct eastward transport of the Loop Current; 3: westward transport by the wind-driven ocean currents on the Campeche Bank; 4: westward transport by the wind-driven ocean currents on the Campeche Bank and eddies; 5: westward transport by the westward propagation of eddies (e.g., Loop Current Eddies or LCEs); 6: westward transport by the relaying of eddies (e.g., LCEs); 7: westward transport by the westward extension of the Loop Current system; 8: westward transport by the westward currents (e.g., coastal currents on the Louisiana–Texas Shelf) with/without eddies in the northern/central GoM.

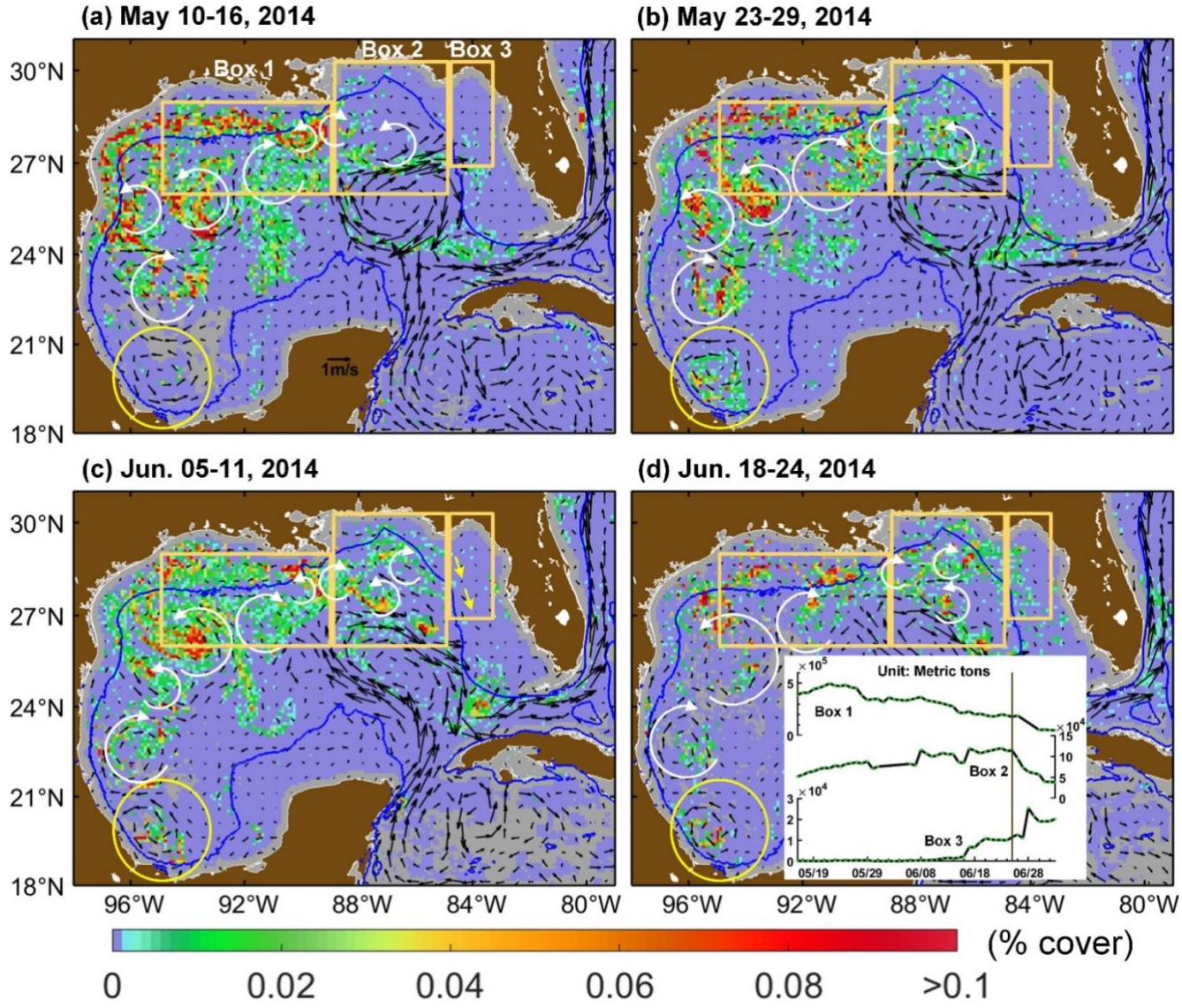

Figure 3. Distributions of MODIS weekly *Sargassum* areal density in the GoM during May and June 2014, showing the eastward transport of *Sargassum* from the northwestern GoM to the eastern GoM. A value of 0.02 on the color bar denotes 0.02%. Gray color indicates no data, and the blue lines represent the 200 m isobath in each figure. Three areas annotated with yellow boxes in each figure were chosen for the time series analysis of *Sargassum* biomass density, and the corresponding results are presented in the inset figure of (d). Note that several consecutive dates (i.e., June 27–29 for box 1 and June 1–5 for box 2) had relatively large cloud cover, thus *Sargassum* biomass density data for these dates over box 1 or box 2 were excluded from the time series analysis. The yellow circle in each figure highlights a cyclonic eddy in the Bay of Campeche. The black vectors (with scale overlaid on land in (a)) represent altimetry-based ocean surface currents in each figure, and the white curves with arrows indicate the eddies located in the western and northern GoM, determined from visual inspections.

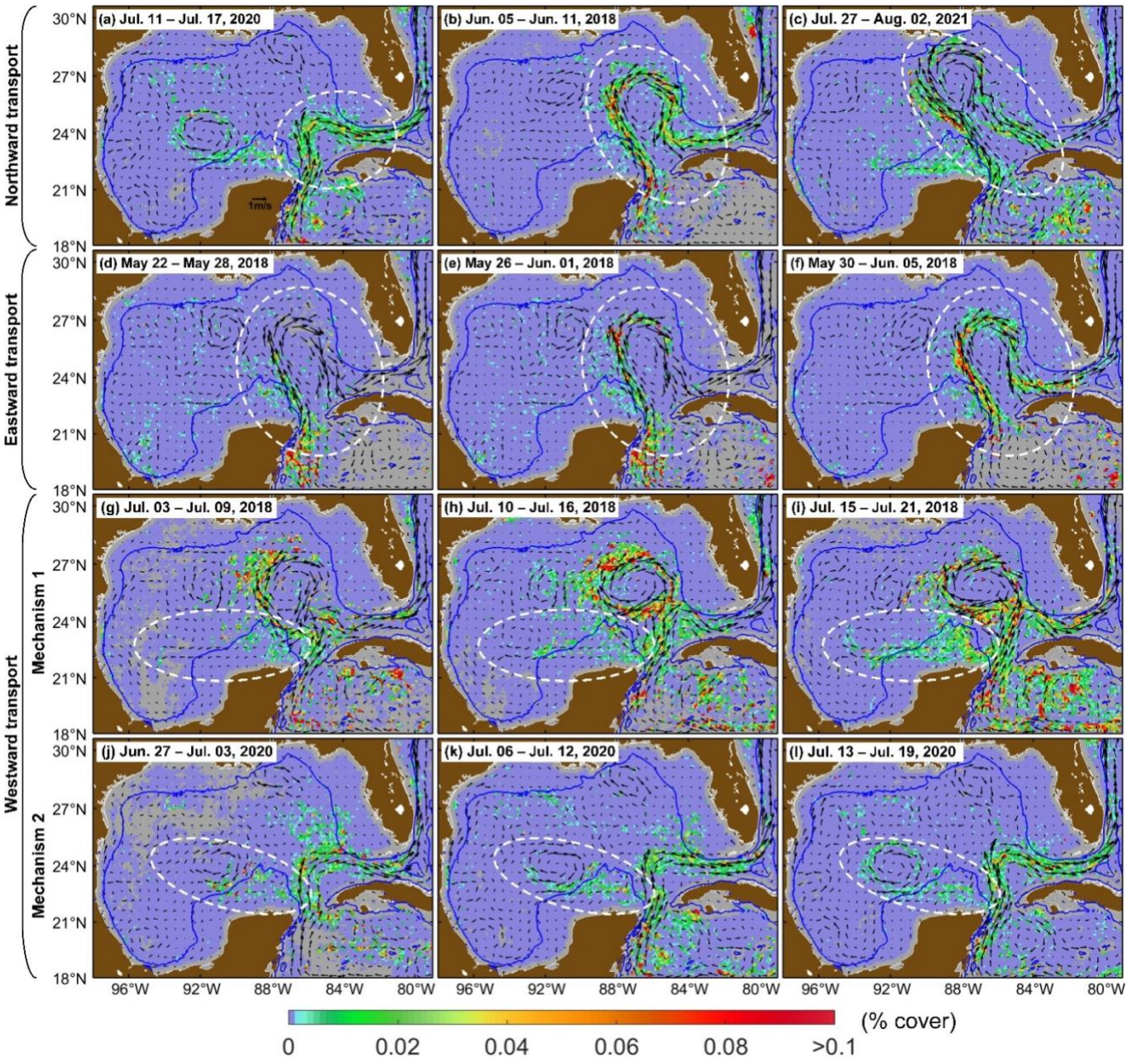

721

722 Figure 4. Distributions of MODIS weekly *Sargassum* areal density in the GoM, showing the
723 northward (a–c), eastward (d–f), and westward (g–x) transport of *Sargassum* of Caribbean origin.
724 A value of 0.02 on the color bar denotes 0.02%. Gray color indicates no data, and the blue lines
725 represent the 200 m isobath in each figure. The dashed white ellipse in each figure highlights the
726 *Sargassum* patterns under physical transport. The black vectors in each figure (with scale shown in
727 (a) and (m)) represent altimetry-based ocean surface currents. Note that dates in (a)–(c) are not
728 sequential.
729

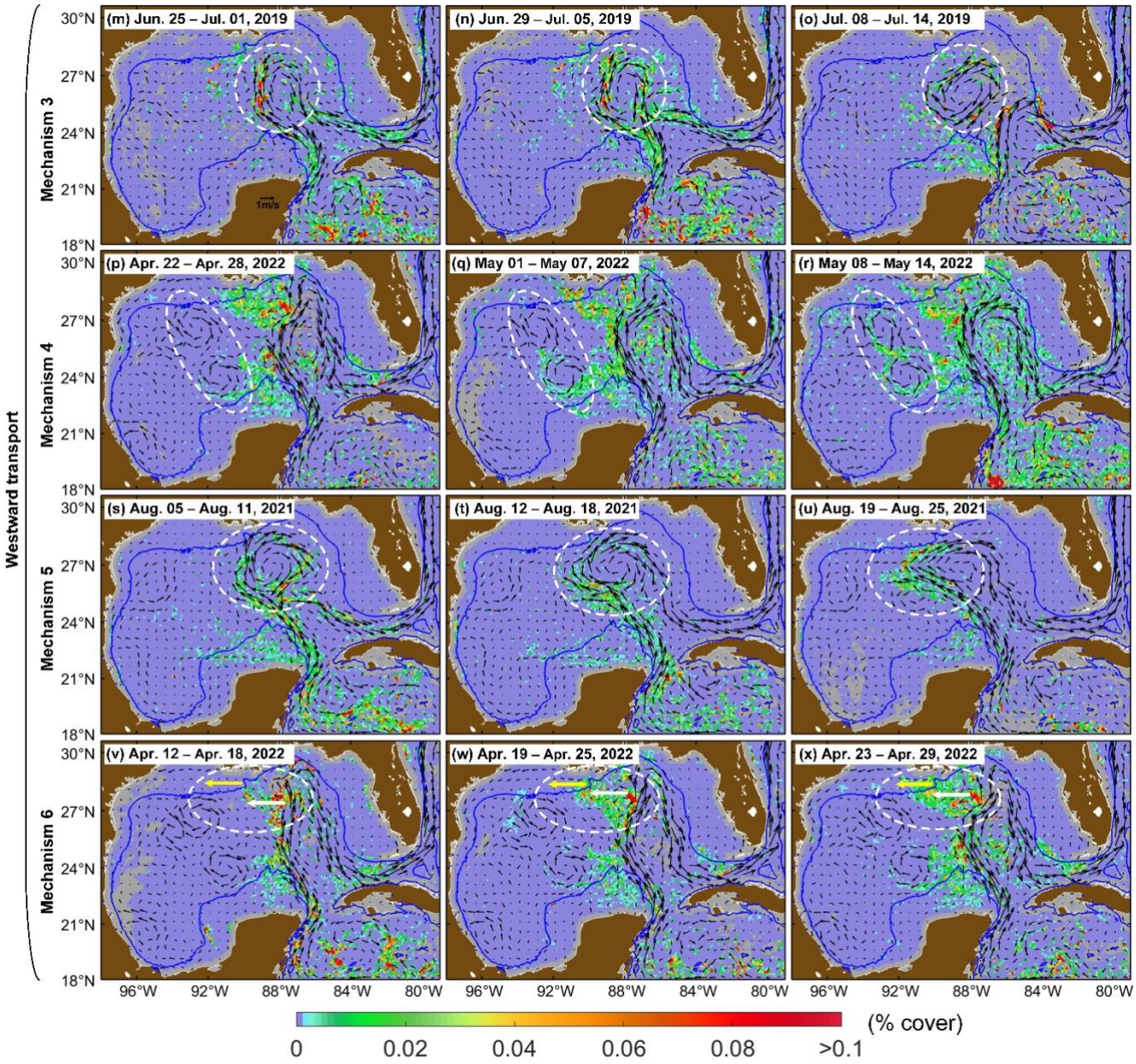

730

731

732 Figure 4. (Continued)

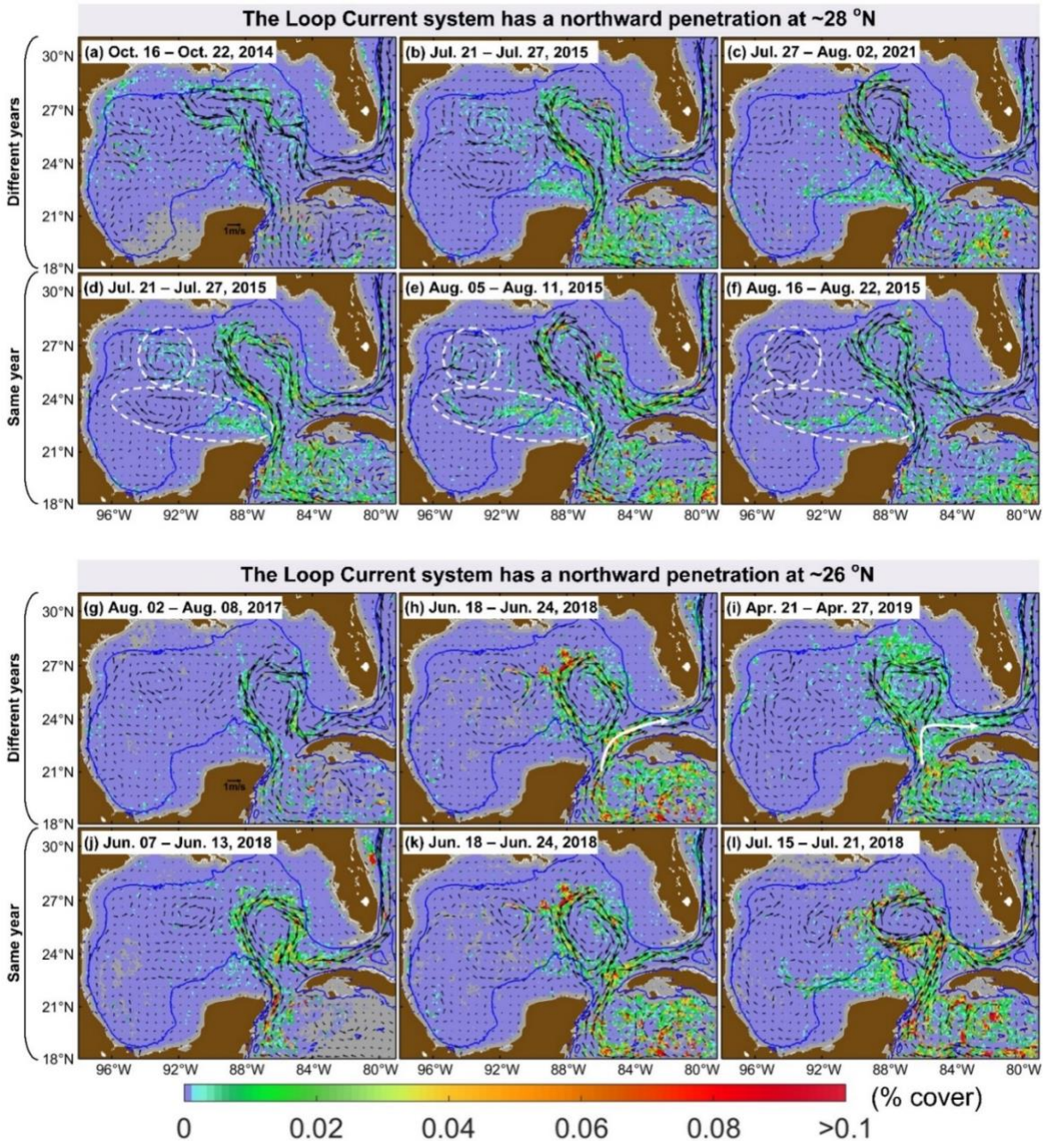

Figure 5. Distributions of MODIS weekly *Sargassum* areal density in the GoM, showing the different spatial patterns of *Sargassum* when the LCS has a northward penetration at ~28ºN (a–f) and ~26ºN (g–l). For the first case (northward penetration at ~28ºN), the *Sargassum* distribution maps are differentiated into different years (a–c) and the same year (d–f). For the other case (northward penetration at ~26ºN), (g–i) and (j–l) show the spatial patterns of *Sargassum* in different years and the same year, respectively. A value of 0.02 on the color bar denotes 0.02%. Gray color indicates no data, and the blue lines represent the 200 m isobath in each figure. The black vectors in each figure (with scale shown in (a) and (g)) represent altimetry-based ocean surface currents. The dashed white circles and ellipses in (d)–(f) highlight two examples of westward transport of *Sargassum*. The white curves with arrows in (h) and (i) indicate the direct transport of *Sargassum* from the northwestern Caribbean Sea to the Straits of Florida.

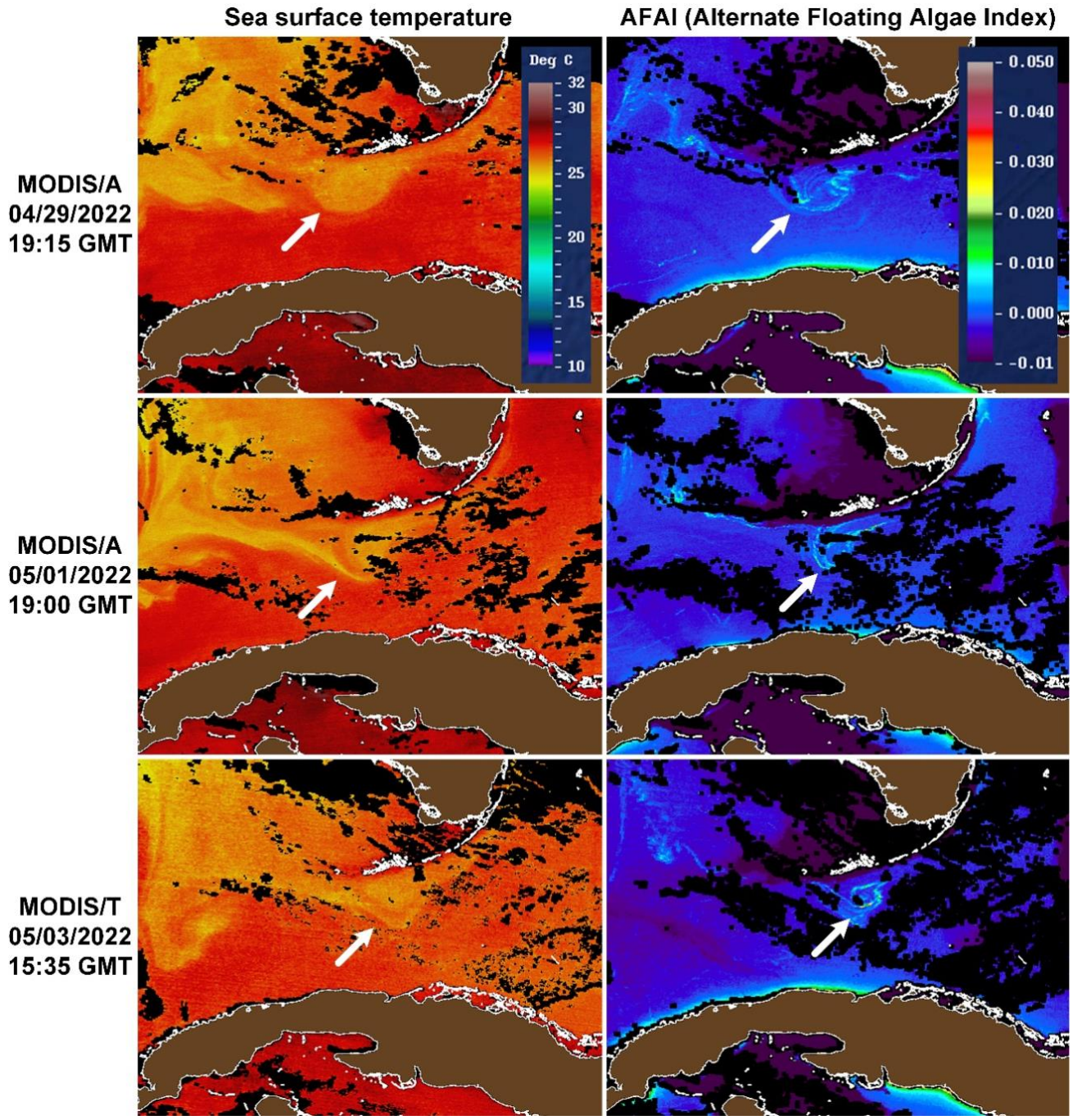

Figure 6. Distributions of MODIS sea surface temperature (unit: °C; left panel) and Alternate Floating Algae Index (AFAI, no unit; right panel) in the Straits of Florida on April 29, May 1, and May 3, 2022, showing the eastward transport of *Sargassum* due to the eastward movement of a cyclonic eddy. The positions of the cyclonic eddy and related *Sargassum* rafts are indicated by white arrows. Black color in each image means no data. These images cover a region of 21.6ºN–26ºN and 84.5ºW–79ºW, and they were obtained from https://optics.marine.usf.edu/cgi-bin/optics_data?roi=GCOOS&current=1.

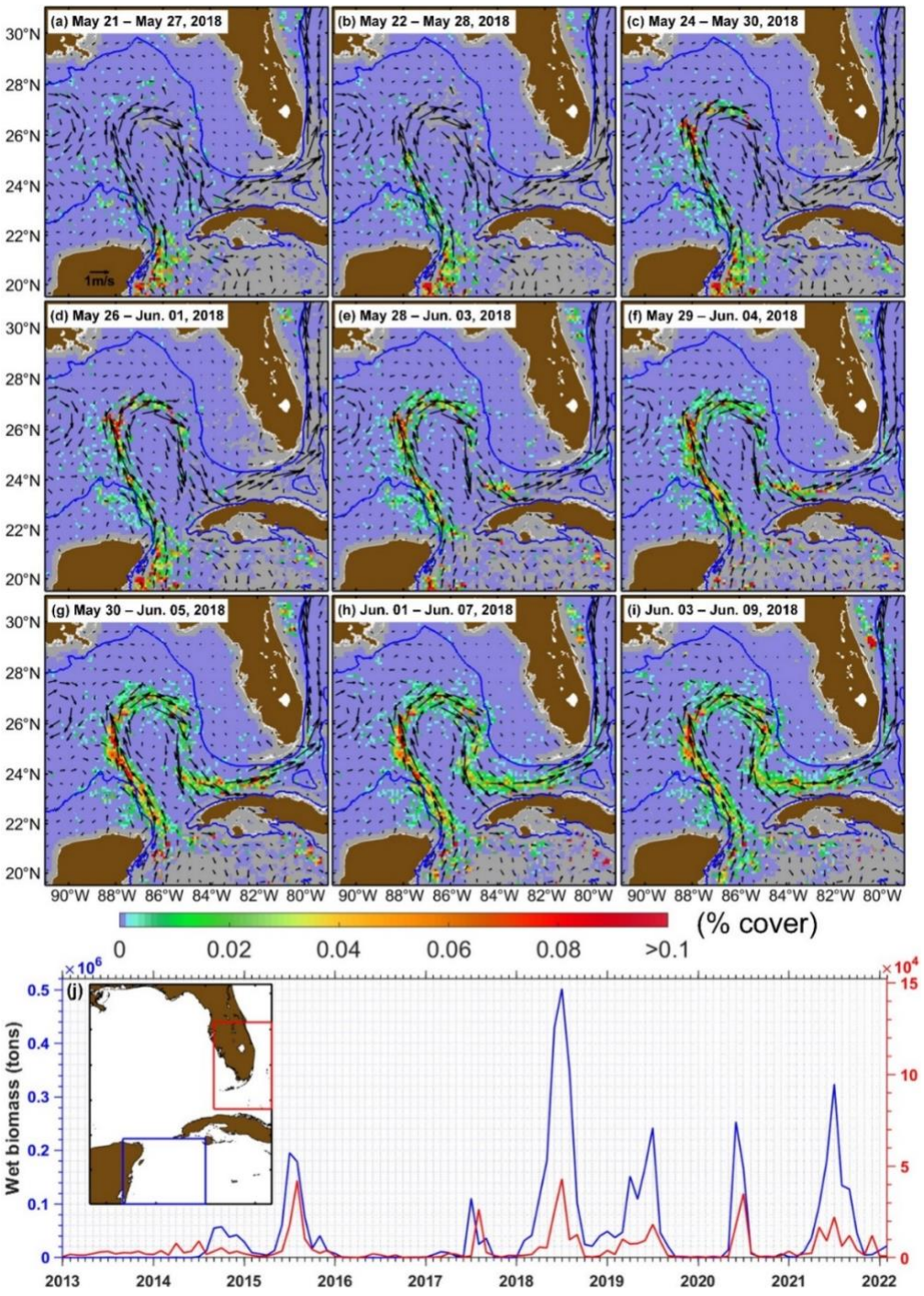

Figure 7. Distributions of MODIS weekly *Sargassum* areal density (a–i), showing an example of continuous transport of *Sargassum* from the northwestern Caribbean Sea to the Straits of Florida. A value of 0.02 on the color bar denotes 0.02%. Gray color indicates no data, and the blue lines represent the 200 m isobath in each figure. The black vectors in each figure (with scale shown in (a)) represent altimetry-based ocean surface currents. (j) shows the time series of wet biomass of *Sargassum* from the northwestern Caribbean Sea (blue color) and southeast coast of Florida (red color) between January 2013 and February 2022, and the year mark starts from January.